PHYSICAL REVIEW B **74**, 041310(R) (2006)

Propagation dynamics of individual domain walls in $Ga_{1-x}Mn_xAs$ microdevices

H. X. Tang,[1] R. K. Kawakami,[2] D. D. Awschalom,[2] and M. L. Roukes[1]
[1]*Condensed Matter Physics and Kavli Nanoscience Institute, California Institute of Technology, Pasadena, California 91125, USA*
[2]*Department of Physics, University of California, Santa Barbara, California 93106, USA*
(Received 3 May 2006; revised manuscript received 20 June 2006; published 31 July 2006)

We investigated the transport dynamics of individual magnetic domain walls by employing electrical measurements in multiterminal $Ga_{1-x}Mn_xAs$ microdevices. Domain wall propagation velocities were deduced from time-of-flight planar Hall measurements between multiple electrical probes of our samples. Domain wall motion induced by both magnetic field and electric currents was systematically investigated. Dependent on the strength of applied in-plane magnetic field, two regimes of domain wall motion, involving thermally assisted flow for low fields and viscous flow for high fields, have been identified. However our data shows no evidence of spin-current induced domain wall motion.

DOI: 10.1103/PhysRevB.74.041310 PACS number(s): 75.60.−d, 75.47.−m, 75.50.Pp, 75.70.−i

Advances in nanofabrication and epitaxial growth provide new levels of resolution and control for the study of magnetic domains at the microscopic level. Previous studies have primarily focused upon thin films of metallic ferromagnetic materials.[1] Dilute ferromagnetic semiconductors, principally $Ga_{1-x}Mn_xAs$, currently attract considerable interest due their promise for unique spintronic devices and ultrahigh density data storage.[2] Intriguing micromagnetic phenomena involving single magnetic domains within $Ga_{1-x}Mn_xAs$ epilayers have recently been reported.[2–6] For example, current-induced domain wall switching has been observed in perpendicularly-magnetized $Ga_{1-x}Mn_xAs$ thin films at modest current densities.[7] To understand the underlying physics in detail, a systematic investigation of the dynamical properties of domain wall (DW) is essential. Such understanding is crucial for engineering a spin transistor or a memory, since these require precise control of magnetization reversal.

Currently, there are several experimental approaches to the study of domain wall (DW) dynamics. One of the most common techniques is time-resolved imaging via the magneto-optic Kerr effect (MOKE),[8–10] an optical method that can provide sufficient contrast to allow direct observation of growth and shrinkage of magnetic domains within a sample. Another recently developed approach is based upon electrical measurements via the giant magnetoresistance (GMR) effect, which has enabled investigations of domain wall propagation in submicron Permalloy wires.[11] In the latter work, the observed $\sim 1\ \Omega$ GMR jumps emanate from regions that are smaller than are readily accessible to MOKE. In this paper, we report a electrically-based approach that enables studies of the dynamics of individual magnetic domain walls. These investigations are enabled by the giant planar Hall effect (GPHE) in $Ga_{1-x}Mn_xAs$.[3] The GPHE-induced resistance change in multiterminal, micron-scale devices patterned from this material can be as large as $100\ \Omega$. This is several orders of magnitude greater than analogous effects previously observed in metallic ferromagnets. Accordingly, our electrical measurements provide very high resolution, sufficient to enable real-time observations of the nucleation and field-induced propagation of individual magnetic domain walls within our monocrystalline devices.

Our samples employ 150 nm thick $Ga_{0.948}Mn_{0.052}As$ (001) epilayers grown on top of an insulating (001) GaAs buffer layer by low temperature molecular beam epitaxy (MBE). These $Ga_{1-x}Mn_xAs$ films are intrinsically magnetized in-plane due to a combination of compressive lattice-mismatch-induced strain and demagnetization effects.[2] The epilayers are subsequently patterned into multiterminal devices, with longitudinal axes, i.e., the direction of current flow, oriented along [110] (a cubic hard axis). Both the fabrication methods and our GPHE-based analysis of the magnetic properties of $Ga_{1-x}Mn_xAs$ epilayers are described elsewhere.[3,12]

Figure 1(a) displays the measurement setup and an electron micrograph of a typical sample. We utilize three pairs of transverse voltage probes separated by 100 μm. Measurements are carried out with a battery supplied, constant dc drive current (1 μA). Induced transverse ("Hall") voltages are coupled through triaxial cables to three low noise, electrically isolated, dc coupled differential amplifiers providing 1 MHz signal bandwidth. A multichannel digital oscilloscope enables simultaneous acquisition of voltage time records from these three signal channels. During measurement, the device temperature is regulated at stepped values between 0.3 K and 45 K (the latter being the Curie temperature of wafer of material from which the devices of this study were fabricated).

A representative *R-H* loop (here *R* is the giant planar Hall resistance) is shown in Fig. 1(b); it is obtained at $T=5$ K with a field oriented 15° away from [110] and ramped at a rate of 15 Oe/s. The first jump corresponds to a magnetization transition from $[0\bar{1}0]$ to [100]; the second jump completes the reversal by switching from [100] to [010]. The square hysteresis loops obtained at low temperatures indicate magnetization switching that is dominated by wall motion, rather than successive domain nucleation.[1] In $Ga_{1-x}Mn_xAs$, except for those directions that are precisely collinear with the easy axes, the magnetization transitions evolve via the formation of a 90°-domain wall.[3,12] In this study we concentrate on time-domain studies of the first transition, which occurs sharply at a rather low switching field and involves initial and final states very close to those at equilibrium in zero field.

The domain wall propagation experiments are carried out by inducing a metastable magnetization state within the sample. This is achieved dynamically by first applying a

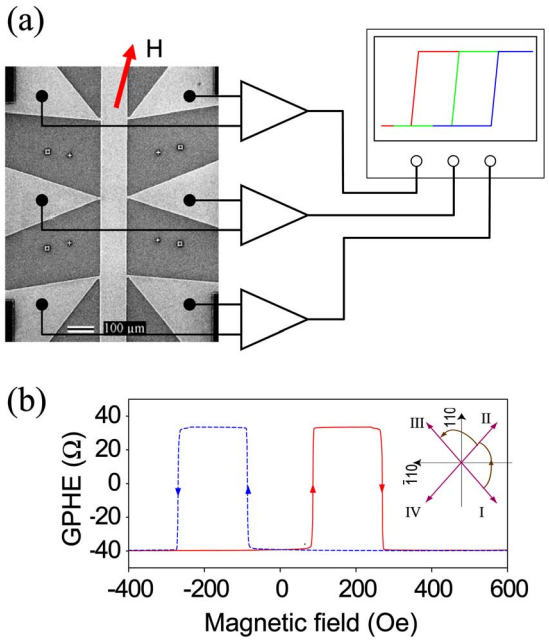

FIG. 1. (Color online) (a) Measurement and sample layout. A constant dc sensing current is driven between top and bottom contacts, which are oriented along [110] in these monocrystalline devices. An external, in-plane magnetic field is applied 15° away from this axis. High input impedance differential amplifiers are used to make potential measurements at three transverse probes. After a domain wall is nucleated at one side of the sample, it propagates sequentially across these transverse probes, successively generating GPHE signal voltages. (b) A typical GPHE resistance (R) vs magnetic field (H) loop for a 100 μm-wide Hall bar at T=5 K.

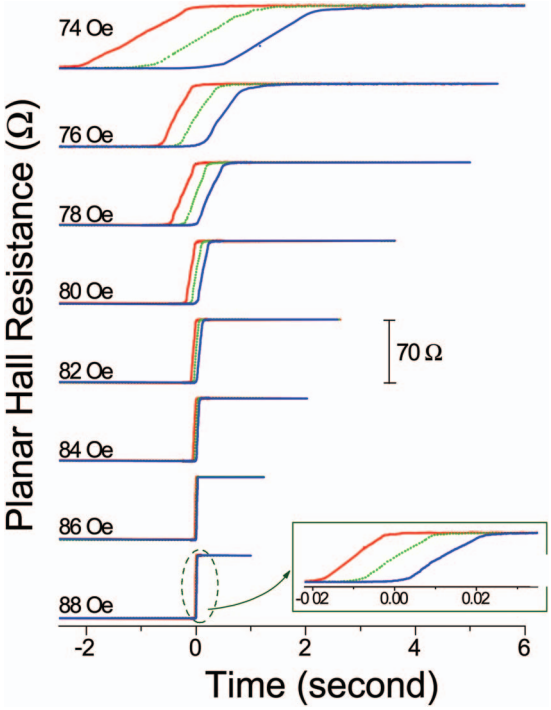

FIG. 2. (Color) GPHE responses obtained at three transverse probes (differentiated by the colored traces), with in-plane field increasing from 74 to 88 Oe at 5 K and 15° from [110] orientation. Inset: A magnified view demonstrates the fast dynamics occurring at 88 Oe.

strong in-plane magnetic field in a selected direction to saturate the magnetization, then smoothly ramping to a specific field magnitude with orientation antialigned to the initial saturation field. At the temperatures studied, domain wall nucleation occurs infrequently through intrinsic stochastic processes. Once nucleated, the constant in-plane field drives growth of the domain possessing magnetization most closely aligned with the applied field. We find that domain wall motion induced in this manner always involves propagation from a wide current contact pad [not shown in Fig. 1(a)] into the channel.[13] With this protocol, completely reproducible signals are detected.

Figure 2 shows the temporal evolution of domain wall propagation, measured via a family of GPHE measurements at 5 K, for in-plane magnetic fields stepped between 74 Oe and 88 Oe. The three simultaneously-obtained time records (of GPHE voltage) reveal a single domain wall's sequential passage along each of the sample's transverse probes. At a given field, the three temporal waveforms have identical magnitudes and transition (i.e., rise) times, but occur with characteristic time delays. The delays between the signal onsets at successive channels are identical, as expected, given the constant interprobe spacing (100 μm). These data are consistent with the picture that domain walls propagate along the device while retaining a fixed shape.[5,6] Domain wall velocity can therefore be extracted by measuring the time-of-flight between transverse probes.

Below 25 K, the data indicate that magnetization reversal proceeds through infrequent nucleation of single domain walls within one of the (large) current contacts, followed by uniform propagation through the device channel. Above 25 K, however, multiple local domain wall nucleation appears to dominate the magnetization reversal process, and our time of flight method is not applicable. Figure 3(a) presents the measured dependence of domain wall velocity on applied in-plane field, for temperatures of 5, 10, and 20 K respectively. Note that the DW velocity spans four decades over this temperature range.

We find that the v-H curves exhibit highly nonlinear dependence upon in-plane magnetic field. This behavior can be divided into two distinct regimes. For driving fields H is larger than a specific threshold H_0 (essentially the intrinsic coercive field), we observe a linear $v \sim H$ relation that is characteristic of viscous flow. The DW velocity in this regime can be expressed as

$$\mathbf{v} = \mu(H - H_0) \tag{1}$$

with μ is the domain wall mobility.[14] This mobility varies strongly with temperature; our data show that it increases from 1.4 mm/s Oe at 5 K to about 14 mm/s Oe at 20 K. These results are summarized in Table I.

Upon reducing the magnetic field well below H_0, the domain wall velocity in our system decays preciptously. We find that our data in this regime are best fit by a model for thermally-activated depinning[15]

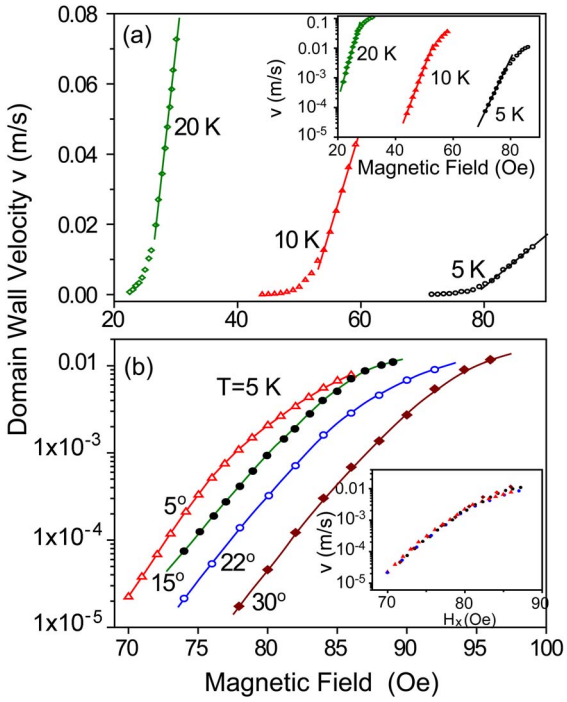

FIG. 3. (Color online) (a) Domain wall velocity as a function of magnetic field at 5 K, 10 K, and 20 K, displayed in linear and semilogarithmic formats (inset). The external field is orientated 15° away from [110]. In the linear plot solid lines represent fits to the high field velocities. In the semilogarithmic plot solid lines are linear fits to the low field region. Each data point represents an average of 20 repeated measurements. (b) Domain wall velocity vs magnetic field orientation. Data are taken at 5 K. Angles are measured with respect to the longitudinal axis of the device. Inset: Domain wall velocity vs field component along [110]. In the inset, data points of different angles condense onto on a single universal curve in the low field regime.

$$\mathbf{v} \propto \exp[(\mathbf{H}\cdot\Delta\mathbf{M}V_N - E_p)/k_BT] \propto \exp[\alpha(H\cos\varphi_H - H_a)]. \tag{2}$$

Here E_p is the activation energy for domain wall propagation, V_N is the activation volume, $\Delta\mathbf{M}=\mathbf{M}_2-\mathbf{M}_1$ (with $\mathbf{M}_1$ representing the initial magnetization (close to $[0\bar{1}0]$) and $\mathbf{M}_2$ the magnetization after switching (close to [100])), φ_H is the magnetic field orientation, the coefficient $\alpha = \sqrt{2}M_SV_N/k_BT$, and the activation field $H_a=E_p/\sqrt{2}M_SV_N$ (here M_S represents the saturation magnetization of $Ga_{1-x}Mn_xAs$). From the low-field slopes of our semilogarithmic curves [Fig. 3(a), inset] we estimate the activation volumes for different temperatures (displayed as a linear dimension, $V_N^{1/3}$, in Table I).

TABLE I. Characteristic parameters determined for GaMnAs in two field regimes.

Temperature (K)	$4\pi M_s$ (G)	Mobility (mm/s Oe)	H_0 (Oe)	α (Oe^{-1})	$V_N^{1/3}$ (nm)
5	493	1.39	79.8	0.185	18.2
10	445	6.11	52.1	0.260	27.4
20	339	14.2	24.8	0.342	42.4

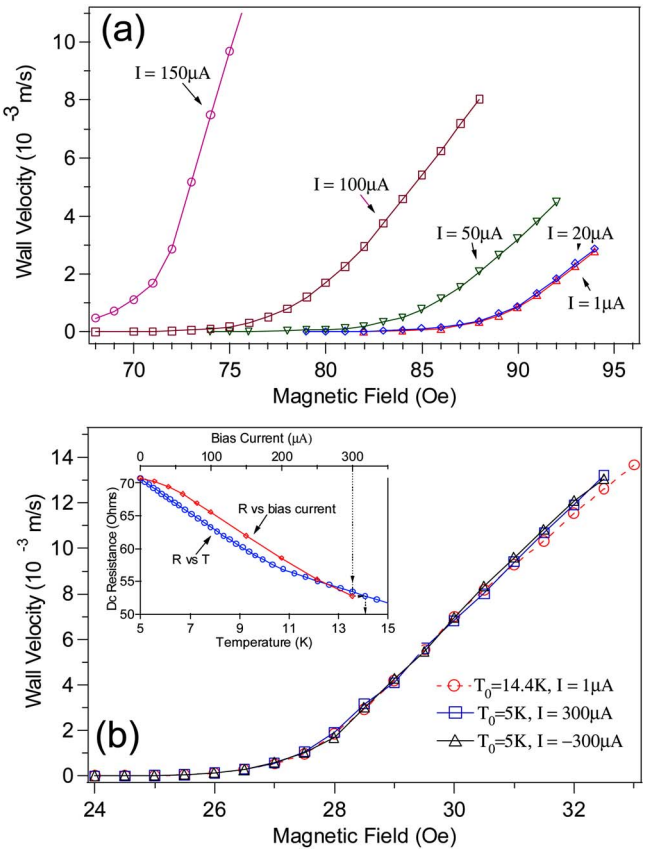

FIG. 4. (Color online) (a) Domain wall velocity dependence on external magnetic field when subject to various dc drive current at 5 K base temperature. The external field is orientated 15° from [110]. Below 20 μA, domain wall motion is insensitive to the biasing current. Higher domain wall velocity is observed at higher bias current. (b) Domain wall velocity measured and compared at positive bias current (300 μA, 5 K base temperature), negative bias current (−300 μA, 5 K base temperature), and the device equivalent temperature (14.4 K). The enhancement of domain wall velocity at higher current density is attributed to the current induced heating effect. *Inset:* Plot of four-terminal dc resistance of the device versus temperature at low bias and versus biasing current at base temperature. These curves are used to determine the effective temperature of the device at constant bias current.

Investigating the v-H curves along various sweep angles further confirms the validity of Eq. (2). Figure 3(b) is the measured dependence of DW velocity on applied field, swept along 5°, 15°, 22°, and 30° orientations. After scaling the magnetic field by cos φ_H, all data within the low field region coalesce onto a single universal curve [Fig. 3(b), inset]. This indicates that it is solely the field component along [110] that is effective for driving domain wall motion.

We have shown that magnetic-field-induced domain wall motion is controllable—in a range of four orders of magnitude by supplying magnetic field of different strengths. However, domain wall motion can be also induced by electric field or electrical current across the domain wall through a

domain drag effect.[16] Such current-induced domain wall motion has been clearly visualized by magnetic force microscopy in metallic systems[17] and by magneto-optic imaging in ferromagnetic semiconductors.[7] It is worth noting that for the semiconductor case the domain wall motion can be driven by a current density of 10^5 A/cm^2,[6] which is two to three orders of magnitude smaller than that required in metals. In this set of experiments we vary the dc bias current in our sample and directly observe domain wall propagation between probes of our multiterminal sample via the GPHE. Figure 4(a) shows the velocity as a function of external magnetic field for several typical values of drive current. Apparently, at higher current densities domain wall velocity is enhanced and the intrinsic coercive field is significantly reduced. Figure 4(b) shows the velocities measured at positive current bias and negative current bias with same current magnitude. Upon reversal of the current flow, in the presence of external magnetic field, the current-induced spin drag effect should reverse sign and induce a domain wall velocity change, whereas the Joule heating remains the same. Up to the highest currents applied in these experiments (300 μA, which corresponds to a current density of 2000 A/cm^2), no significant change in domain wall velocity is observed upon reversal of the current flow. These observations appear to be different from what has been seen previously. We believe that the enhanced rate of domain wall motion at higher current densities originates from Joule heating; at elevated temperatures higher domain wall mobility is expected. Data of the inset of Fig. 4(b) appear to demonstrate this; they show the temperature dependence of the four-teminal resistance R_{xx} at $I=1$ μA and the current dependence of R_{xx} at a base temperature of 5 K. Ignoring the fact that electrical heating induces in a nonuniform temperature field within the sample, comparison of the two curves suggests that the effective device "temperature" roughly increases to $\sim$14.4 K for a 300 μA drive current. With this established, we ramp the base temperature to 14.4 K and measure the domain wall velocity at much lower current, i.e., 1 μA, where heating is negligible. The corresponding velocity data, reproduced in Fig. 4(b) as circles, match the velocity curves obtained for both positive and negative bias currents at the maximum applied value of this study (300 μA). These observations confirm that the effects we observe are due to heating: the current-induced domain wall motion at 300 μA is not discernible above the temperature-induced changes to DW velocity.

Note that at the maximum current we have applied in our low temperature measurements, the applied current density (2000 A/cm^2) is well below the critical current (8×10^4 A/cm^2) found in Ref. 7 for current induced domain-wall switching within perpendicularly magnetized $Ga_{1-x}Mn_xAs$ at 82 K. Here, by biasing a longitudinally-applied magnetic field far beyond the intrinsic coercive field, our approach should allow us to resolve current-induced domain wall switching at significantly lower current densities.[18] Such events are not observed. However, it is notable that the single domain walls in the present study possess 90° *in-plane* domain structure. The interactions of this type of DW with the magnetic field and electrical current may be different from those of the 180° Bloch-like DWs studied in previous work.[7]

Our domain wall time-of-flight measurements between electrical contacts of mutliterminal $Ga_{1-x}Mn_xAs$ devices, allow a new avenue for the investigation of the individual domain wall dynamics. This domain wall motion is susceptible to both applied magnetic field and electrical current, and measurements of this provides qualitative insights to the underlying mechanisms driving domain wall motion in these interesting dilute magnetic semiconducting materials.

We acknowledge support from DARPA under grants DSO/SPINS MDA 972-01-1-0024 (Caltech) and DARPA/ONR N00014-99-1-1096 (UCSB), and from the AFOSR under grant F49620-99-1-0033 (UCSB).

[1] J. Ferré, Top. Appl. Phys. **83**, 127 (2002).
[2] H. Ohno, Science **281**, 951 (1998).
[3] H. X. Tang, R. K. Kawakami, D. D. Awschalom, and M. L. Roukes, Phys. Rev. Lett. **90**, 107201 (2003).
[4] S. Das Sarma, Nat. Mater. **2**, 292 (2003).
[5] H. X. Tang, R. K. Kawakami, D. D. Awschalom, and M. L. Roukes, Nature (London) **431**, 52 (2004).
[6] H. X. Tang and M. L. Roukes, Phys. Rev. B **70**, 205213 (2004).
[7] M. Yamanouchi, D. Chiba, F. Matsukura, and H. Ohno, Nature (London) **428**, 539 (2004).
[8] S. B. Choe and S. C. Shin, Phys. Rev. Lett. **86**, 532 (2001).
[9] S. Lemerle, J. Ferré, C. Chappert, V. Mathet, T. Giamarchi, and P. LeDoussal, Phys. Rev. Lett. **80**, 849 (1998).
[10] D. A. Allwood, D. A., G. Xiong, M. D. Cooke, C. C. Faulkner, D. Atkinson, N. Vernier, and R. P. Cowburn, Science **296**, 2003 (2002).
[11] T. Ono, H. Miyajima, K. Shigeto, K. Mibu, N. Hosoito, and T. Shinjo, Science **284**, 468 (1999).
[12] H. X. Tang, Ph.D. Dissertation, Caltech (2002).
[13] K. Shigeto, T. Shinjo, and T. Ono, Appl. Phys. Lett. **75**, 2815 (1999).
[14] T. H. O'Dell, *Ferromagnetodynamics: The Dynamics of Magnetic Bubbles, Domains, and Domain Walls* (John Wiley & Sons, New York, 1981).
[15] M. Laurune, S. Andrieu, F. Rio, and P. Bernstein, J. Magn. Magn. Mater. **80**, 211 (1989).
[16] J. C. Deluca, R. J. Gambino, and A. P. Malozemoff, IEEE Trans. Magn. **MAG-14**, 500 (1978).
[17] A. Yamaguchi, T. Ono, S. Nasu, K. Miyake, K. Mibu, and T. Shinjo, Phys. Rev. Lett. **92**, 077205 (2004).
[18] T. Kimura, Y. Otani, K. Tsukagoshi, and Y. Aoyagi, J. Appl. Phys. **94**, 7947 (2003).